NUCIRC simulation of a large header for the CANDU* type nuclear reactor heat transport system.

A. Kwan [1,2], R. Dam [1], M. Soulard [1], G.D. Harvel [1], V.S. Krishnan [1]

1. Atomic Energy of Canada Limited, Sheridan Park, Mississauga, Ontario, L5K 1B2
2. Department of Engineering Physics, McMaster University, Hamilton, Ontario, L8S 4M1

Abstract

A header manifold model for the NUCIRC code has been developed for the large scale CANDU type nuclear reactor. NUCIRC's header manifold model was originally designed for the CANDU 6 heat transport system (HTS) [1,2], but is modified in this work to extend it to a large scale system. The large scale CANDU system uses parallel core passes with a common reactor outlet header (ROH), and is designed to accommodate 100 more fuel channels than the CANDU 6 design [3,4].

Two different reactor header models can be employed in the NUCIRC code: the non-manifold and the manifold model. The non-manifold model simulates the reactor headers as constant pressure reservoirs [5]. The manifold model possesses the ability to capture the differences in the header designs, and the axial pressure gradients in the reactor headers due to the flow distributions along the headers. As a result, the manifold model should provide a more accurate predictions on the flow channels header-to-header pressure drops. This paper will demonstrate the ability of the header manifold model to better simulate the large scale CANDU reactor by generating a more detailed representation of the HTS when compared to the non-manifold model.

Introduction

Since an increase in output may lead to a better return on the capital investment, the larger scale CANDU reactor examined in this paper is designed to accommodate 100 more fuel channels than the CANDU 6 system [3,4,6]. Hopefully, this will translate to a reduction in the unit energy cost and therefore a better rate of return [4].

Thermalhydraulics modelling is very important for nuclear reactor designs and operational supports. Consequently, the NUCIRC simulation code is developed to better predict the CANDU HTS operating parameters under different initial conditions. NUCIRC is originally designed for the CANDU 6 HTS [1,2], but the code employed in this paper is modified to simulate the larger scale CANDU system. A schematic of the larger scale CANDU HTS is illustrated in Figure 1.

The non-manifold header model simulates the CANDU reactor headers (both inlet and outlet) as constant pressure reservoirs [5]. Although this model does produce adequate results, experimental data have shown that axial pressure gradients exist in the reactor headers, which give rise to distinct header-to-header pressure drops for each fuel channels [2]. Since the header-to-header pressure drop is directly related to the channel flow rate, and the channel flow is used to compute the critical channel power (CCP) [7], precise

* CANDU (CANada Deuterium Uranium) reactor is a trademark of AECL.

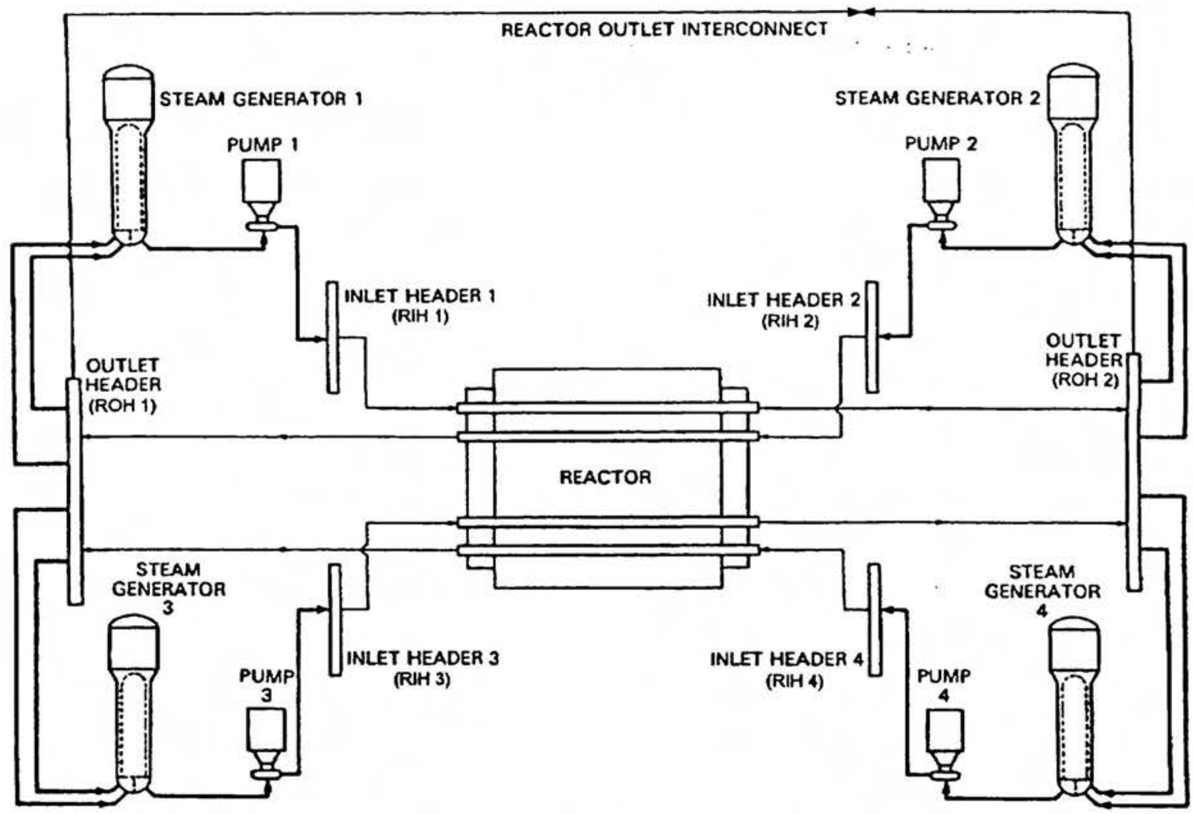

Figure 1: Schematic of the larger scale CANDU reactor HTS
(based on Figure 2 in Reference 6)

determination of the header-to-header pressure drop for each flow channel is of utmost importance. Consequently, the manifold model has been developed for the CANDU headers. In reference 2, the manifold model has demonstrated its effectiveness in the CANDU 6 system and in a generic header design. It is the purpose of this paper to extent this model to the larger scale CANDU type header.

Methodology

A manifold may be described as a flow channel with a number of openings at the side wall (lateral branches) in which the fluid can enter or leave [8]. While simulation of the manifold may be performed using the energy or the momentum balance equation, the energy equation, in the form of the Bernoulli equation, can not be easily applied due to the difficult in choosing the correct streamline [2,8]. Therefore, the momentum model developed by Bajura and Jones [9] is utilized in NUCIRC.

In the Bajura and Jones model [9], the equation for the inlet header can be stated as:

$$\frac{1}{\rho}\frac{d\bar{P}}{dx}+\left(\frac{f\,\omega}{8\,A_1}+\frac{d\beta}{dx}\right)\bar{V}^2+\theta\,\bar{V}\frac{d\bar{V}}{dx}=0 \quad (1)$$

where ρ is the density of the fluid, P is the pressure, x is the distance along the header, f is the Moody friction factor as predicted by Colebrook-White, ω symbolizes the cross sectional perimeter of the inlet header, A is the cross sectional area of the inlet header where the subscript "1" denotes the main flow channel, β is the axial flow momentum correction factor, V is the velocity and θ is defined as:

$$\theta = 2\beta - \gamma \qquad (2)$$

Here γ is the lateral flow momentum correction factor through the cross-sectional area of the feeder pipe (A_3). The lateral flow momentum correction factor (γ) can be computed by:

$$\gamma = \frac{1}{\overline{V}\,\overline{V}_3 A_3}\int_{A_3} V_x V_y \, dA_3 \qquad (3)$$

where the subscript "3" represents the feeders or lateral branches. The $\overline{V}$ is the average velocity, while V_x and V_y is the x and y velocity components of the fluid at feeder pipe respectively. In addition, the axial flow momentum correction factor (β) can be accounted for as follows:

$$\beta = \frac{1}{\overline{V} A}\int_{A} V^2 \, dA \qquad (4)$$

Finally, the equation for the outlet (or combining) header is the same as Equation 1 except for a negative sign in front of the Moody friction factor (f). This is required because the coolant in the reactor outlet header is flowing in the opposite direction of the inlet header.

Currently, each reactor inlet header is divided into 2 sections, while each reactor outlet header is divided into 8 different sections. The reason for the creation of two manifolds (or sections) under each riser is that manifold has flow in a single axial direction, and the fluid flow in a given inlet header is in two axial directions. Conversely, each outlet

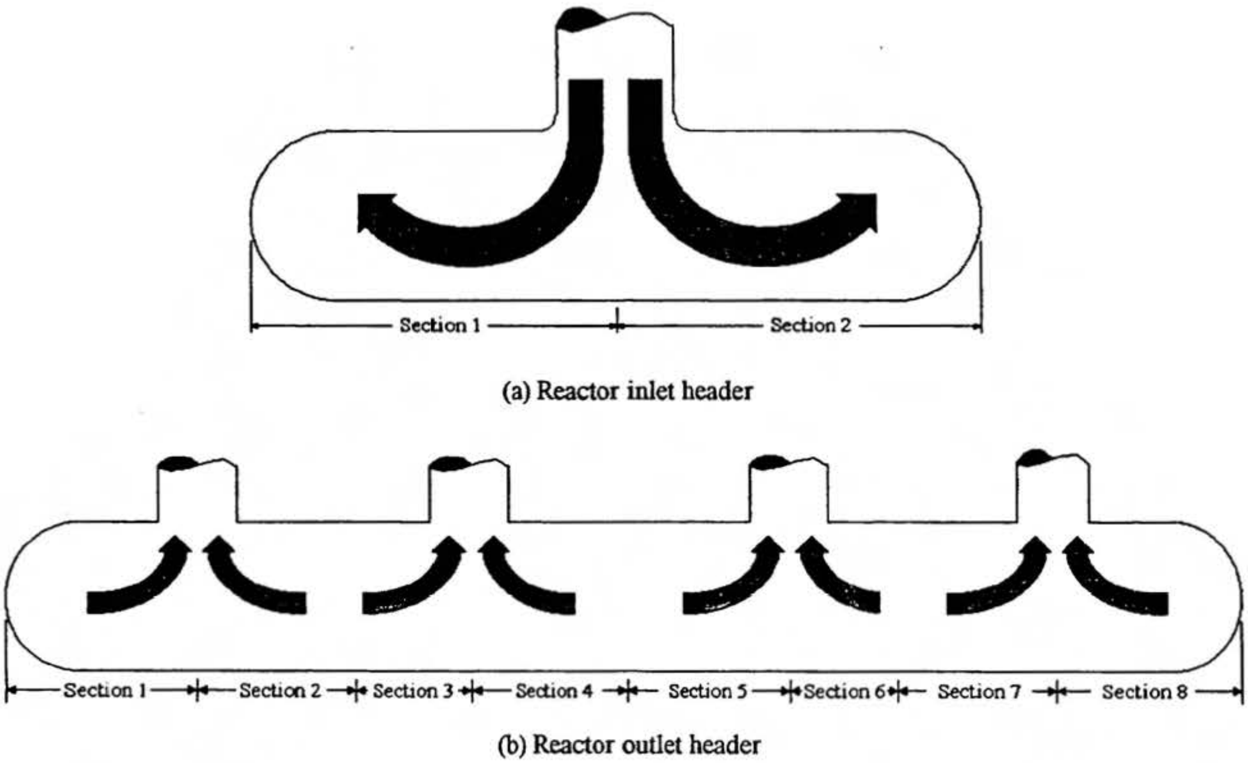

Figure 2: Flow distribution in the typical large CANDU reactor headers

riser can receive flows from two different axial directions. Figure 2 demonstrates the flow distribution in the typical large CANDU type reactor headers. Figure 2a also shown that the coolant flow in the inlet header may not be full developed in the first few planes of the inlet header. This presents the need for the momentum correction factor.

For solution purposes, each of these sections is considered as an individual manifold with its own flow and pressure distribution. However since these manifolds are not completely independent of each other, NUCIRC must incorporate the relationships between these manifolds to correctly simulate the whole header. This can be accomplished by matching the pressure of different sections at a common point like the inlet of the steam generator, or at a common plane between sections.

Convergence Criteria

Since the manifold model divided the outlet header into eight sections, the pressure in each of these sections will need to be adjusted independently in order to achieve pressure convergence. To aid in the pressure convergence computation, the outlet header and its risers is separated into different regions as shown in Figure 3. Due to the fact that the outlet header pressure, the inlet header pressure and the flow rate (header-to-header pressure drop) are interdependent, an outlet header pressure convergence can be achieved only if both the inlet header and the flow rate are also converged. Therefore, only a check on the outlet header pressure is required.

To start the pressure convergence adjustment for the outlet headers, pressure in Section 1 of the reactor outlet headers (P_{S1}) is assumed to be the reference pressure. For the outlet header in the first half (or pass) of the HTS (ROH2), P_{S1} is calculated by matching it to the pressurizer node pressure. For the second half of the HTS (ROH1), P_{S1} is adjusted so that the mass flow rate convergence is attained. This convergence check is needed because the mass flow rate for each fuel channel is computed independently. Once the pressure of Section 1 is computed, the convergence between P_{S1} and P_{S2} is based on the pressure at riser 1 (P_{R1}). Next, the convergence between P_{S1} and P_{S3} is based on the steam generator inlet plenum pressure (P_{SG1}). Finally, the convergence between P_{S3} and P_{S4} is based on P_{R2}.

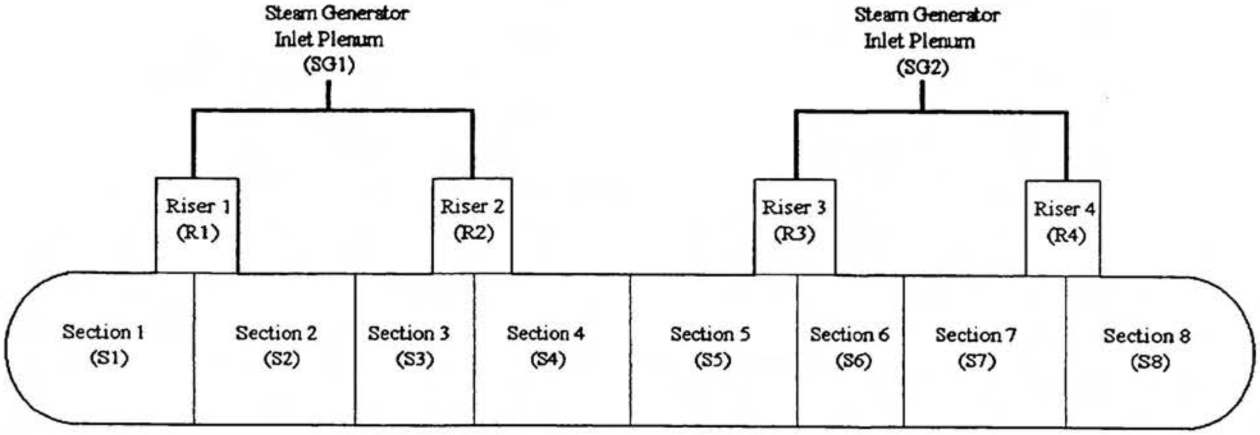

Figure 3: The location of the different sections on the reactor outlet header

The pressure adjustment for Section 5 to 8 is similar to Section 1 to 4. The pressure of Section 5 is taken as the reference pressure, and it is adjusted relative to P_{S1} based on the flow split fraction convergence (below). The flow split fraction (α) is used to split the coolant flow at the outlet header since two independent sets of external circuit are attached to each reactor outlet header (Figure 1). Next, the convergence between P_{S5} and P_{S6} is based on P_{R3}, and the convergence between P_{S5} and P_{S7} is based on P_{SG2}. Finally, the convergence between P_{S7} and P_{S8} is based on P_{R4}.

Since the mass flow for each fuel channel is computed independently, a flow split fraction convergence check is needed to ensure the mass flow rate exiting the outlet header into the external circuit is equal to the mass flow rate entering the inlet header downstream. Here α is the flow split fraction at the outlet header and ϕ is the fractional mass flow rate entering the downstream inlet header. For each pass, ϕ for only one of the two inlet headers is calculated because the flow split fractions from a given reactor outlet header should be complementary.

Due to the law of conservation of mass, the mass flow entering the steam generator must be the same as the mass flow entering the inlet header downstream as mentioned above (This assumption is valid since the current model does not account for the purification injection flow, the reactor outlet header balance line or the loop by-pass flow). Consequently, the following convergence criteria are developed:

$$\frac{\phi_{RIH3}}{\alpha_3} = 1.0 \tag{5}$$

and,

$$\frac{\phi_{RIH4}}{\alpha_4} = 1.0 \tag{6}$$

where, the subscript on α indicates the flow is entering the external circuit upstream of the given inlet header number. The errors for the ratios above (Equations 7 and 8) are taken as the differences between the calculated ratio (left hand side of the equations) and one. The tolerance for these ratios are currently set at 0.001 (0.1%), but may be adjust by the user to any value greater than 1×10^{-8} if desired.

If the error on the ratio is greater than the tolerance, then the pressure at Section 5 of the respective outlet header is adjusted. This will lead to the pressure adjustment of subsequent sections (Sections 6, 7 and 8) as discussed above. The quadratic method, which correlates the variations between the inputted (guessed) pressure and the outputted (calculated) pressure in the last three iterations to produce a better estimate of the inputted pressure for the next iteration, is utilized for this adjustment.

The energy (or heat balance) is the final variable NUCIRC needs to converge to achieve a steady-state solution. In the current method, the tolerance is set to be 0.1% of the total power produced by the second pass. That is if the power left over from the second half of the HTS is less than 0.1% of the total power generated in the pass, convergence is achieved. Otherwise, a secant method is used to adjust the temperature. In order to apply the secant method, the average temperature of the two headers is calculated. Once the average temperature is computed, the following secant method is applied:

$$T_{avg}^{new} = \frac{E^{cur} \times T_{avg}^{old} - E^{old} \times T_{avg}^{cur}}{E^{cur} - E^{old}} \tag{7}$$

where the subscript "*avg*" represents the average temperature of the two inlet headers in the first half of the HTS. The variable E symbolizes the power (or enthalpy) left over in the second half of the HTS. This new average inlet header temperature is then used to determine the new inlet header temperatures by adding or subtracting half of the difference between the two old inlet header temperatures to the average value.

Results and Discussion

The reactor inlet and outlet header pressures for the 60% and 100% of full fuel channels power are plotted in Figure 4 to 7 for comparison. From Figure 4, one can observe that differences between the manifold results for the first inlet header design (RIH1 and RIH2) are larger than the non-manifold results, while the differences between the manifold results for the second inlet header design (RIH3 and RIH4) are smaller than the non-manifold model. One of the reasons for the differences is the different pressure convergence methods used by the models. The non-manifold model needs to adjust the whole header pressure for headers in only the first pass in order to achieve pressure convergence, while the manifold model will adjust the section(s) of the outlet header in all of the passes (which is a better reflection of the actual situation). As a result, the pressures predicted by the two models will be different.

In an ideal case, the pressure for the header with the same design should be the same. However, differences in the feeder geometry and inlet header designs make this a non-ideal simulation. A similar effect is observed in Figure 5 for 100% full power inlet header case, but this time the differences in pressure for inlet headers is on average larger than the 60% full power case. One possible explanation for this is the variation in computation due to the change in energy. Another possible explanation is numerical (round-off) error.

Another observation from Figure 4 and 5 is that the manifold model tends to predict a higher inlet header pressure than the non-manifold model. This is caused by the smaller nozzle losses for the non-manifold model (The nozzle loss coefficients for the non-manifold model are inputted by the user, while the nozzle loss coefficients for the manifold model are calculated on-line by NUCIRC). Subsequent simulations (not shown) utilizing the averaged nozzle loss values from the manifold model as the inputted nozzle loss coefficients for the non-manifold model resulted in better agreement between the manifold and the non-manifold inlet header pressure.

From Figure 4 and 5, one may also observed that the predicted header pressure is slightly different between the two inlet header designs (the second design on average has a lower header pressures), and contains two more channels (planes). This demonstrates the ability of the manifold model to capture the differences in the header designs.

Finally from Figure 4 and 5, one may observe that the inlet header pressure increases in the positive flow direction. This demonstrates the ability of the manifold model to capture the axial pressure gradients in the inlet headers due to the flow distribution, and therefore provides more accurate predictions of the channel's header-to-header pressure drops.

When comparing the large inlet header results in Figure 4 and 5 with the CANDU 6 inlet header results [2], one may noticed that a couple of the pressure peaks observed in the CANDU 6 header is missing in the large inlet header results. One possible explanation is that those pressure peaks in the CANDU 6 inlet header occurs in the feeders located right underneath the inlet riser. Since the large CANDU inlet headers contain no feeders underneath the inlet riser, the results will not reflect such important pressure effect. Consequently, this section of the header is plotted as dots as shown in Figure 4 and 5 to indicate the situation.

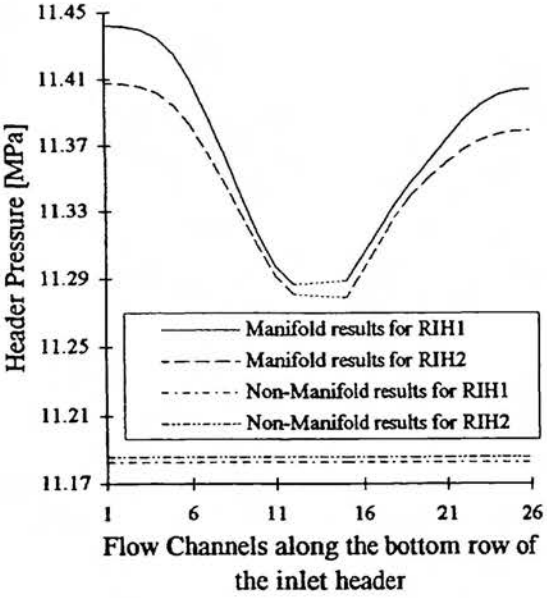

(a) First inlet header design

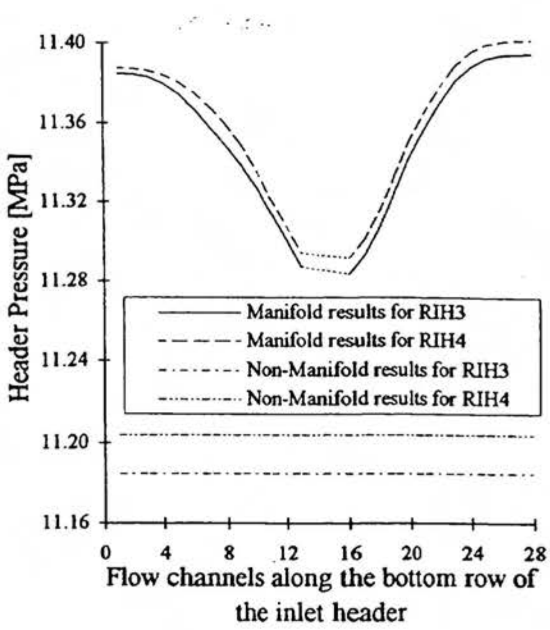

(b) Second inlet header design

Figure 4: Comparison of the calculated non-manifold and manifold inlet headers pressure for the 60% full power case

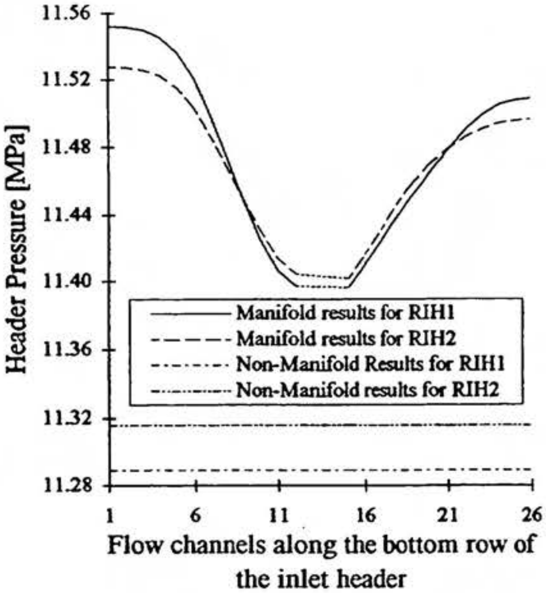

(a) First inlet header design

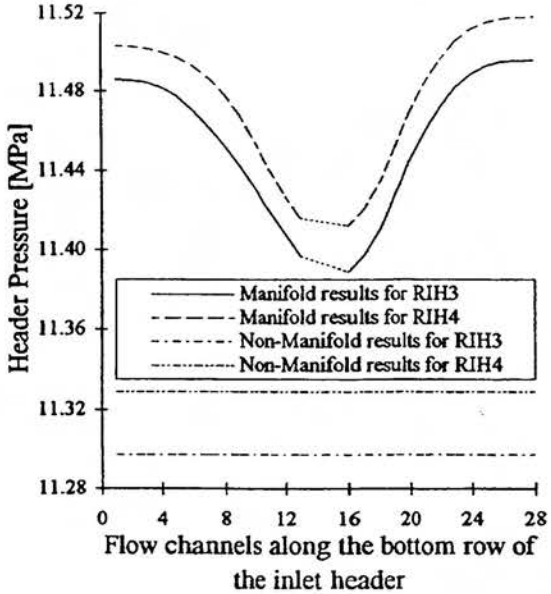

(b) Second inlet header design

Figure 5: Comparison of the calculated non-manifold and manifold inlet headers pressure for the 100% full power case

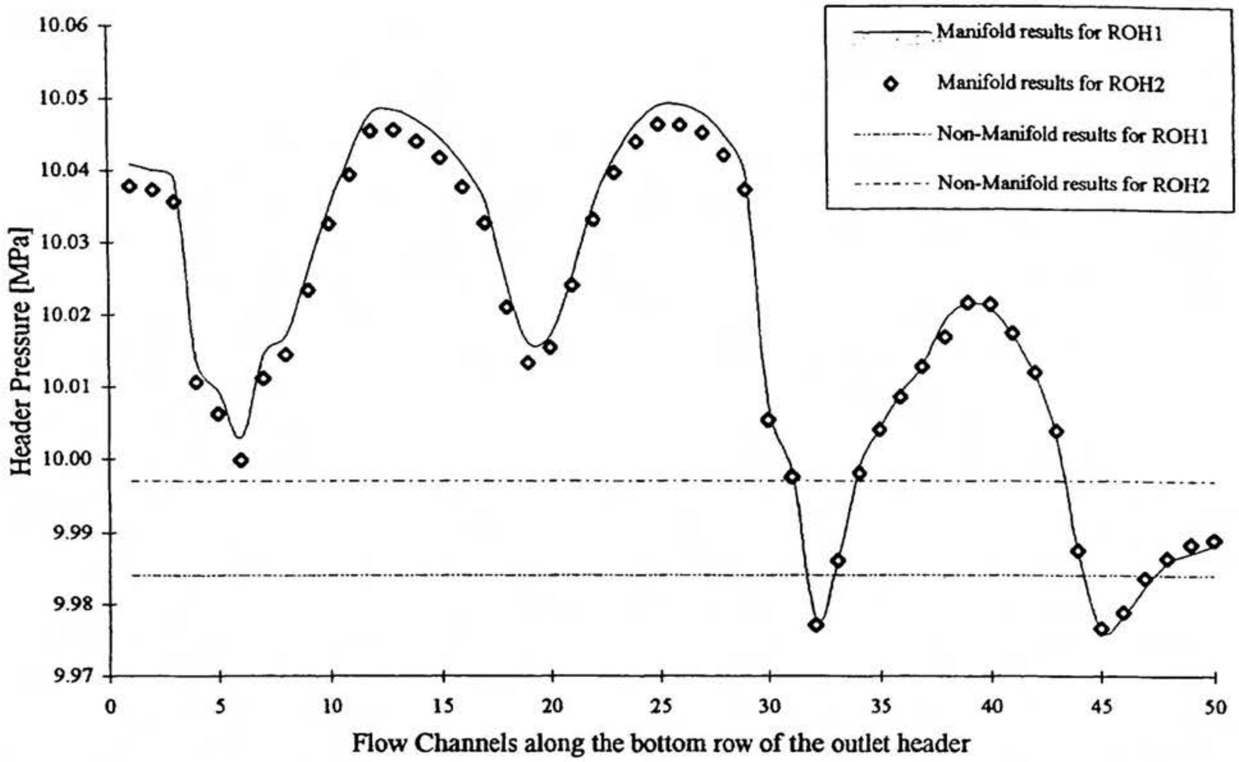

Figure 6: Comparison of the calculated non-manifold and manifold outlet headers pressure for the 60% full power case

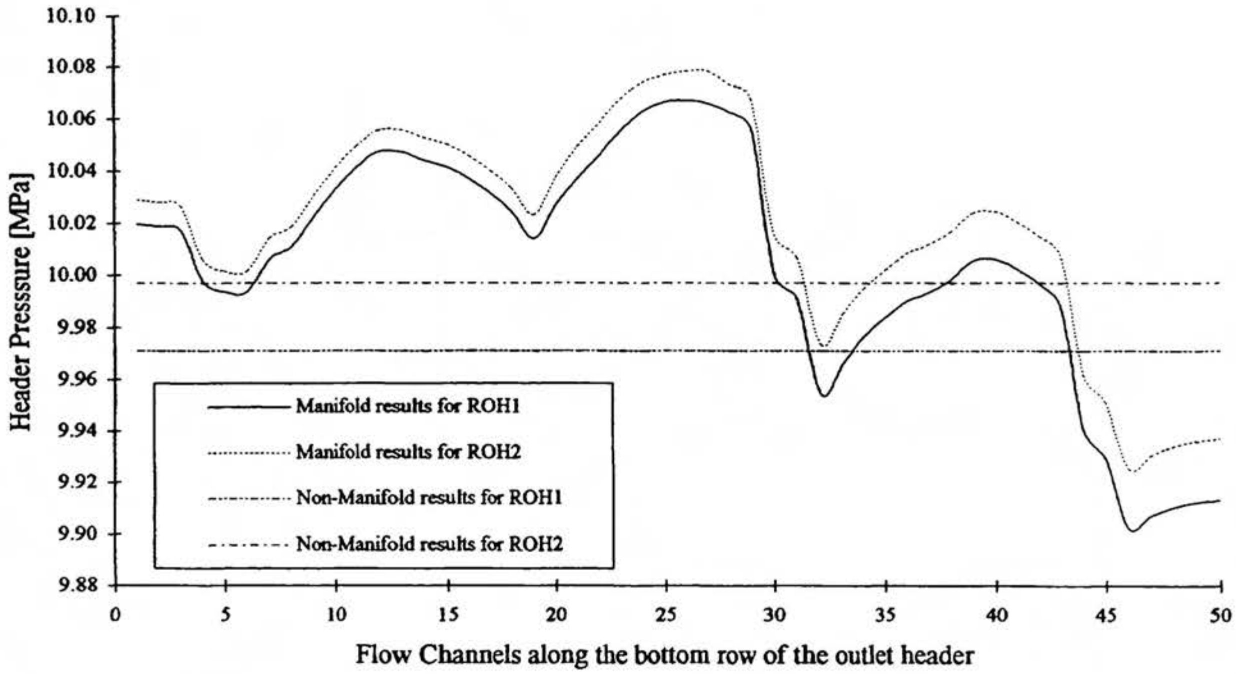

Figure 7: Comparison of the calculated non-manifold and manifold outlet headers pressure for the 100% full power case

Similar conclusions can be drawn from Figure 6 and 7 for the outlet headers at 60% and 100% full fuel channel power cases, although the header pressure decreases in the positive flow direction in the reactor outlet header due to the opposite flow direction. From those two figures, one may observe the following: 1) A smaller difference is observed for the manifold results for ROH1 and ROH2 when compared to the non-manifold results for both power levels; 2) a larger difference between the two reactor outlet headers is observed for the 100% full power case; and 3) the differences in the header pressures for different flow channels from the manifold results demonstrate the ability of the manifold model to capture the axial pressure gradients in the outlet headers.

Conclusion

1. The differences in header-to-header pressure drop between the manifold results of the same header design (both inlet and outlet) are on average smaller than the non-manifold results.
2. The manifold model tends to predict a higher inlet header pressure due to the smaller nozzle losses utilized in the non-manifold model.
3. The differences in the results of the same header design for both models may be attributed to the differences in feeder geometries, which may be accented by the two phase flow at higher power levels.
4. The manifold model possess the ability to capture the differences in the header designs and the axial pressure gradient in the headers.

Future Work

Since the current manifold model employed by NUCIRC did not include the angular effect on the header-to-header pressure drop for the individual feeders (flow channels), one may wish to expand the next generation model to account for this dependence.

Reference

1. M.R. Soulard and K.F. Hau, "Recent Model Development in NUCIRC and Application to CANDU-6 Heat Transport System Performance Evaluation", *CNS Nuclear Simulation Symposium*, Saint John, N.B., August 1991.
2. G.D. Harvel, M. Soulard, R. Dam, P. White, R. Moffet and G. Hotte, "NUCIRC Simulations of A CANDU-TYPE Header Manifold Model", *Fifth CNS International Symposium on Simulation Methods in Nuclear Engineering*, Montreal, Quebec, 1996.
3. G. Brooks, "CANDU Technology-Meeting Future Needs", *Nucl. Energy*, **20** : 409, 1981.
4. K. Hedges, S. Yu and I. Hastings, "Future CANDUs influence the present", *Nuclear Engineering International*, **40** : 42, 1995.
5. A. Kwan, "Simulation of large scale non-manifold header model for the CANDU nuclear reactor primary heat transport system", *22nd CNA/CNS Annual Student Conference*, Fredericton, New Brunswick, March 1997.
6. W.J. Garland and S.H. Pang, "CANDU-600 Heat Transport System Flow Stability", *Nuclear Technology*, **75** : 239, 1986.
7. M.R. Soulard, R.F. Dam, M.B. Carver, J.C. Kiteley, G. Hotte, and R.A. Gibb, "Investigation into the Modelling of the Effect of Pressure Tube Creep on CHF, Dryout Power, and Pressure Drop", *CNS Annual Conference*, Saskatoon, Saskatchewan, 1995.
8. A.B. Datta and A.K. Majumdar, "A calculation procedure for two phase flow

distribution in manifold with and without heat transfer", *Int. J. Heat Mass Transfer*, **9** : 1321, 1983.
9. R.A. Bajura and E.H. Jones, Jr., "Flow Distribution Manifolds", *Transactions of the ASME Journal of Fluids Engineering*, 654, 1976.